$CoCrPt-SiO_2$ granular-type longitudinal media on Ru underlayer for sputtered tape applications

Hwan-Soo Lee,[a] Jian-Gang Zhu, and David E. Laughlin
Data Storage Systems Center, Department of Electrical and Computer Engineering, Carnegie Mellon University, Pittsburgh, Pennsylvania 15213, USA

(Presented on 6 November 2007; received 13 September 2007; accepted 4 February 2008; published online 24 March 2008)

$CoCrPt-SiO_2$ films for use as thin film tape media have been investigated. Bias sputtering and high Ar pressure were utilized to achieve desirable media properties (good in-plane orientation and enhanced grain decoupling) in these media. The in-plane orientation of the bias sputtered $CoCrPt-SiO_2$ magnetic layer was well maintained even at a high content of SiO_2 as Ru was used as an underlayer and deposited at high Ar pressure. Films of (10.0) textured $CoCrPt-SiO_2$ on a Ru underlayer showed a large in-plane coercivity of 4000 Oe and transmission electron microscopy revealed an average grain size of about 10 nm, well decoupled by the oxide. The in-plane coercivity was a strong function of the Ru thickness. © *2008 American Institute of Physics*.
[DOI: 10.1063/1.2885068]

I. INTRODUCTION

Along with candidates proposed in the advanced metallic particle or advanced metal evaporated tape media families, low transition noise sputtered media that can be deposited at room temperature on polymeric substrates will have a major impact on the future of tape storage.[1–3]

$CoCrPt-SiO_2$ perpendicular media fabricated without heating has been shown to produce fine grains that are decoupled by SiO_2 grain boundaries, leading to low noise performance in disk drive media.[4] This approach is appealing for *longitudinal* tape media because it is produced with no heating, in contrast to the well established Cr segregation mechanism. However, tailoring desirable media properties (of in-plane orientation and well-decoupled small grains) with no heating is still a challenge.[5–7]

Previously, we investigated $CoCrPt-SiO_2$ tape media on NiAl/CrMn/CoCrTa underlayers in terms of recording performances and physical properties.[7] The SiO_2 content was optimized not to disturb the preferred Co (10.0) grain orientation. Better grain isolation in the magnetic layer would be, however, in need to improve the linear density further.

In the present paper, $CoCrPt-SiO_2$ films on Ru underlayer (stack A) have been investigated in comparison with $CoCrPt-SiO_2$ on NiAl/CrMn/CoCrTa (stack B). We found the Ru underlayer functions better as an underlayer to induce high in-plane anisotropy in the $CoCrPt-SiO_2$ layer while pertaining to well-separated small magnetic grains. In conjunction with the use of Ru underlayer, in fabricating the magnetic layer, two notable features of bias sputtering and high Ar pressure were utilized to modify the film microstructure and attain better grain isolation.[8,9]

II. EXPERIMENTAL

$CoCrPt-SiO_2$ films were prepared on two different underlayer stacks by rf diode sputtering in a Leybold–Heraeus Z-400 system with no oxygen added to argon gas. Stacks A and B are schematically shown in Fig. 1. The two composite underlayer stacks were used to produce the in-plane texture in the $CoCrPt-SiO_2$ layer. The $CoCrPt-SiO_2$ films for stack A were deposited on a two step Ru underlayer [substrate/Ta (5 nm)/Ru1 (10 nm)/Ru2 (45–75 nm)]. This was performed by changing argon (Ar) sputtering pressure during deposition. Ar pressure for the Ru1 and Ru2 layers was 5 and 30 mTorr, respectively. In some cases, the Ru1 layer was left out since the insertion of the Ru1 was not very critical. For stack B, substrate/NiAl (60 nm)/CrMn (30 nm)/CoCrTa (10 nm)/$CoCrPt-SiO_2$ films were prepared. The sputtering pressure for NiAl, CrMn, and CoCrTa was 10 mTorr.

The Ar sputtering pressure for the magnetic layer of stacks A and B was varied in a range between 5 and 40 mTorr. The thickness for the magnetic layer was typically between 15 and 20 nm. Substrate bias was utilized to change morphology during the magnetic film growth.[8] The substrate bias was only applied for the magnetic layer and in a range between −100 and −130 V. No intentional substrate heating was applied. Rigid substrates (either Si or glass) were largely used for better reproducibility, but the magnetic properties on polymeric substrates [aromatic polyamide (ARAMID)] were presented in the text as well. A mean roughness (R_a) of the polymeric substrate was 1.4 nm, within a 5×5 μm^2 region.

The film composition (in at. %) was determined by inductively coupled plasma analysis. Film textures and microstructures were characterized by an x-ray diffractometer

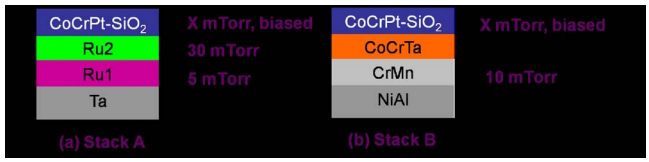

FIG. 1. (Color online) Typical sample structures and relevant deposition conditions. Stack A: Ta (5 nm)/Ru1 (8 nm)/Ru2 (45–75 nm)/$CoCrPt-SiO_2$ (15–20 nm) and stack B: NiAl (60 nm)/CrMn (30 nm)/CoCrTa (10 nm)/$CoCrPt-SiO_2$ (15–20 nm).

[a]Electronic mail: hwansoo@ece.cmu.edu.

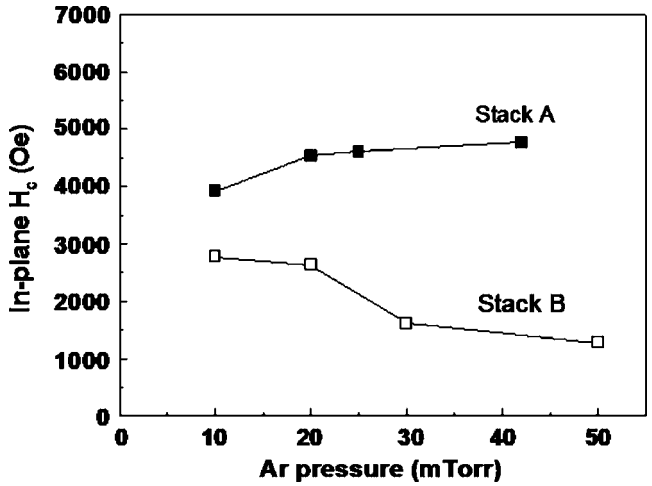

FIG. 2. In-plane coercivity of the CoCrPt–SiO_2 oxide composite films fabricated on different underlayer structures: (a) Si (substrate)/Ru1/Ru2/CoCrPt–SiO_2 (stack A) and (b) Si (substrate)/NiAl/CrMn/CoCrTa/CoCrPt–SiO_2 (stack B).

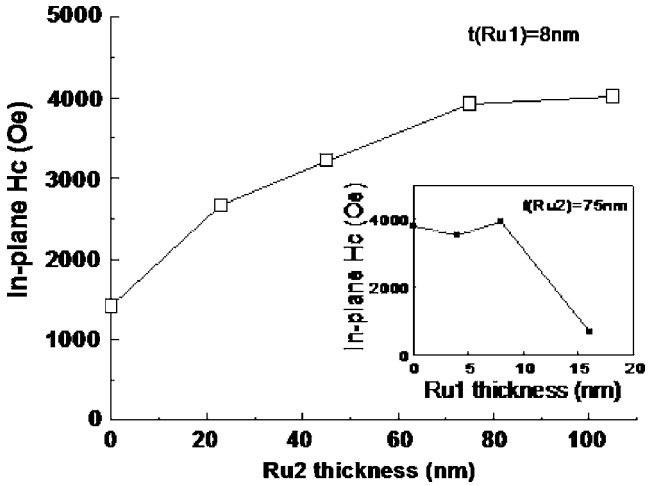

FIG. 4. In-plane H_c as a function of Ru2 thickness. The Ru1 thickness was fixed to 8 nm. The inset shows a variation in in-plane coercivity as a function of Ru1 thickness. The Ru1 layer greater than 8 nm led to the strong Ru (00.2) out-of-plane texture and resulted in significantly low in-plane H_c.

(Philips X'pert Pro with x-ray lens) using Cu $K\alpha$ radiation and by a JEOL JEM-2010 transmission electron microscope (TEM) operating at 200 kV.

III. RESULTS AND DISCUSSION

In Fig. 2, in-plane H_c was plotted as a function of Ar pressure for stacks A and B. Ar pressure and bias voltage were utilized to modify the film microstructure, as in Ref. 9 Interestingly, a notable decrease in H_c for stack B was observed with an increase in Ar pressure, whereas the H_c for stack A remained similar and even slightly increased. We attribute this to an argon pressure dependence of Co (10.0) in-plane orientation, which will be discussed below.

For these samples, grain size was large (~13 nm) particularly at a low Ar pressure of 10 mTorr since biasing has an effect of reducing the amount of oxide in the growing films and promoting the growth of larger grains.[10] However, a higher Ar pressure with biasing greatly helped to reduce grain size smaller than 10 nm and exhibited a much better defined SiO_2 on the thicker boundary.[9] Consistent with this, ΔM measurements indicated a smaller exchange coupling for samples fabricated at a higher Ar pressure. The Pt content was adjusted to have a maximum in H_c at a substrate bias of −120 V. Bias voltage was determined not to degrade the H_c of the magnetic layer, maintaining a small intergranular exchange coupling ($\sim\Delta M < 0.2$).

In Fig. 3, x-ray diffraction (XRD) spectra for stacks A and B are shown. The use of higher Ar pressure during deposition shifted the CoCrPt (10.0) in-plane texture to the right for the two stacks. This can be associated with a change in Pt content as Ar pressure increased. It was observed that the Pt content decreased from 29 to 25 at. % as Ar pressure increased from 10 to 40 mTorr. However, this does not account for the observed trend in Fig. 2.

At these compositions (in at. %), the in-plane lattice parameter of the dimensions for the Ru (10.0) and the CoCrPt (10.0) is very similar. This suggests that for stack A, higher Ar pressure helps to reduce the effect of lattice mismatch between the underlayer Ru (10.0) and the CoCrPt–SiO_2 (10.0) magnetic layer as the Pt content was decreased due to higher Ar pressure. The CoCrTa cell on the (10.0) plane is 0.253×0.409 nm^2 while the Ru cell on the (10.0) plane is 0.270×0.428 nm^2. The $CoCr_{17}Pt_{25}$ cell on the (10.0) plane is 0.265×0.423 nm^2.

Additionally, note that for stack A, the strong Ru (10.1) and Ru (00.2) reflections are present. The high Ar pressure of 30 mTorr for the Ru2 underlayer led to a random orientation in Ru layer. The deposition rate for the Ru2 was 16 nm/min, which nearly doubled that of the Ru1. Interestingly, there appears to be no notable CoCrPt (10.1) or CoCrPt (00.2) c-axis out-of-plane texture, which was also confirmed with the grazing incidence XRD. In support of the above, the low out-of-plane coercivity of 410 Oe was observed whereas the corresponding in-plane coercivity was 4770 Oe.

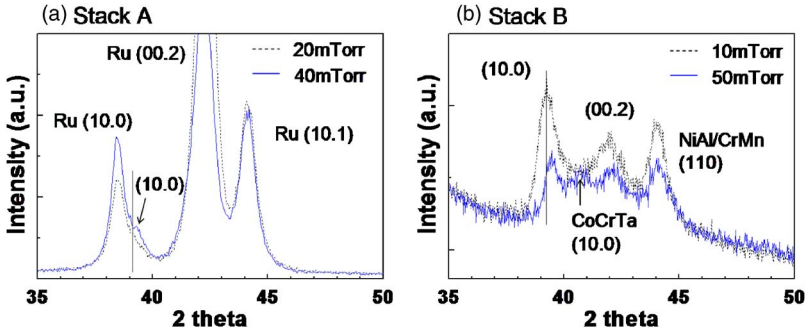

FIG. 3. (Color online) XRD spectra for stacks A and B: (a) Si (substrate)/Ru1/Ru2/CoCrPt–SiO_2 and (b) Si (substrate)/NiAl/CrMn/CoCrTa/CoCrPt–SiO_2. Higher Ar pressure during the deposition of the CoCrPt–SiO_2 magnetic layer shifted CoCrPt (10.0) peak to the right.

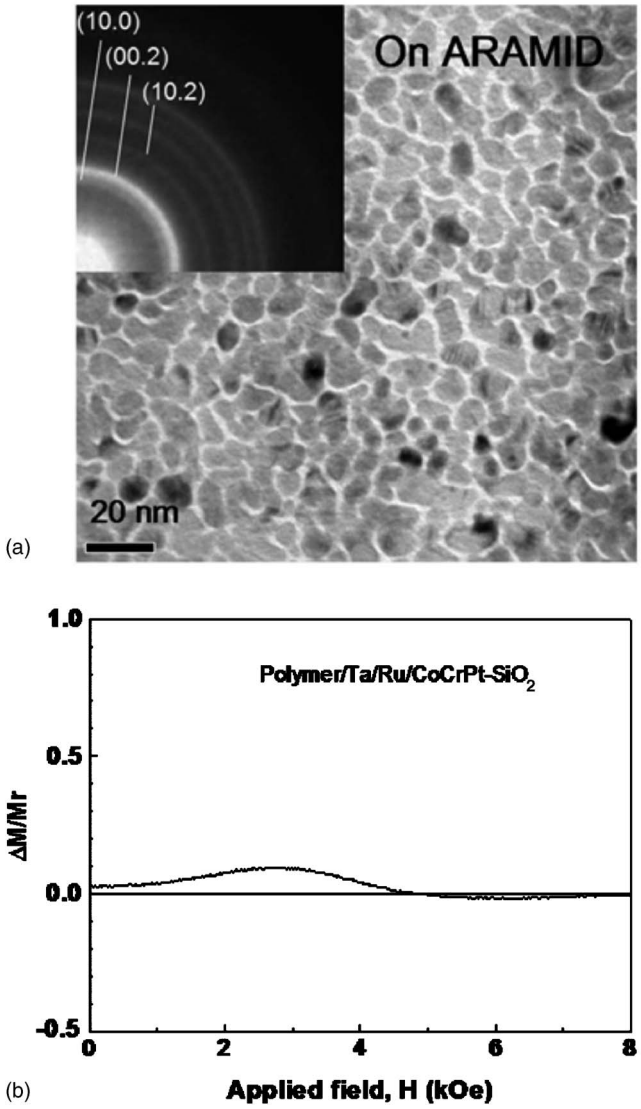

FIG. 5. (a) Plan-view TEM image of ARAMID/Ta (5 nm)/Ru (45 nm)/CoCrPt–SiO_2 (14 nm). The inset indicates selected area electron diffraction (SAED) of the corresponding CoCrPt–SiO_2 layer. (b) The corresponding ΔM curve for the tape media. The tape media exhibits a small positive ΔM (~0.1), suggesting weak exchange coupling in the magnetic layer.

In the remainder of this report, stack A was further characterized in terms of structural and magnetic properties. Figure 4 shows in-plane coercivity H_c of the CoCrPt–SiO_2 films deposited on Si substrates as a function of Ru2 thickness. For this investigation, the magnetic layer was deposited at an Ar pressure of 10 mTorr. Magnetic layers deposited at higher Ar pressure also showed the similar trend. With increasing the Ru2 thickness, a large increase in H_c was observed. This can be attributed to the enhanced Co (10.0) texture with increasing the Ru2 thickness. Note that the Ru1 thickness greater than 8 nm degraded the Co (10.0) texture and resulted in a low in-plane H_c, as indicated by the filled square in the inset. Note also that the insertion of the Ru1 layer is not very critical to obtain high coercivities, however, the presence of the Ru1 layer seems to be helpful in suppressing the CoCrPt (00.2) out-of-plane component.

The role of SiO_2 in grain decoupling can be clearly seen in Fig. 5, where the CoCrPt–SiO_2 (15 nm) films were deposited on polymeric substrates (ARAMID). The similar deposition conditions discussed above were used for the film fabrication on ARAMID except that the Ru1 layer was not present. The Ru underlayer thickness was 45 nm and the Pt content in the magnetic layer was about 25 at. %. The in-plane H_c of CoCrPt–SiO_2 film on polymeric substrates was typically 20%–30% lower, compared to that of the film on rigid substrates.

Figure 5(a) shows a plan-view TEM image and the corresponding selected area electron diffraction (SAED). The average grain size is about 10 nm and the grains are well decoupled by SiO_2 grain boundaries. The SAED pattern shows a weak (10.0) ring of Co with a strong (00.2) reflection, indicating the prominence of the (10.0) texture of CoCrPt–SiO_2 layer.

The corresponding magnetic properties are shown in Fig. 5(b). The oxide tape medium has a coercivity H_c of 3.0 kOe and a peak $\Delta M/M_r$ of ~0.1. We attribute the low ΔM to apparent physical separation between grains in the films. The SiO_2 phase is most likely in the boundaries, providing magnetic isolation. The sheared M-H slope was also observed. For longitudinal disk media, CoCrPtTa or CoCrPtB films displaying weak intergranular interactions as deposited at an elevated temperature, typically showed a ΔM of ~0.1.[11]

IV. CONCLUSIONS

In summary, we have discussed CoCrPt–SiO_2 thin films for advanced tape media applications. The Co alloy-oxide granular-type media is seen to be the media of choice for tape applications owing to the fact that magnetic grain isolation can be achieved by using a nonheating process. It is possible to reduce the intergranular magnetic coupling of longitudinal CoCrPt–SiO_2 media having small grains of about 10 nm without degrading the magnetic properties by selecting suitable underlayer and sputtering conditions.

[1] R. M. Palmer, M. D. Thornley, H. Noguchi, and K. Usuki, IEEE Trans. Magn. **42**, 2318 (2006).
[2] H.-S. Lee, L. Wang, J. A. Bain, and D. E. Laughlin, IEEE Trans. Magn. **41**, 654 (2005).
[3] H.-S. Lee, D. E. Laughlin, and J. A. Bain, IEEE Trans. Magn. **40**, 2404 (2004).
[4] T. Oikawa, M. Nakamura, H. Uwazumi, T. Shimatsu, H. Muraoka, and Y. Nakamura, IEEE Trans. Magn. **38**, 1976 (2002).
[5] K. Moriwaki, K. Usuki, and M. Nagao, IEEE Trans. Magn. **41**, 3244 (2005).
[6] L. Wang, H.-S. Lee, Y. Qin, J. A. Bain, and D. E. Laughlin, IEEE Trans. Magn. **42**, 2306 (2006).
[7] H.-S. Lee, T. Sato, H. Ono, L. Wang, J. A. Bain, and D. E. Laughlin, IEEE Trans. Magn. **43**, 3497 (2007).
[8] H.-S. Lee, J. A. Bain, and D. E. Laughlin, Appl. Phys. Lett. **90**, 252511 (2007).
[9] H.-S. Lee, V. W. Guo, J.-G. Zhu, and D. E. Laughlin, J. Appl. Phys. **103**, 07F541 (2008).
[10] H.-S. Lee, J. A. Bain, and D. E. Laughlin, J. Appl. Phys. **99**, 08G910 (2006).
[11] Y. Kubota, L. Folks, and E. E. Marinero, J. Appl. Phys. **84**, 6202 (1998).